Journal of Heat and Mass Transfer Research

Journal homepage: https://jhmtr.semnan.ac.ir

Semnan University

ISSN: 2383-3068

Research Article

Thermal Performance of CuO-Water Nanofluid Flows Within a Wavy Channel Under the Influence of an External Magnetic Field

Amar Nekbil *, Ahmed Lamine Boukhalkhal, Lakhdar Aidaoui, Yahia Lasbet

Laboratory of Development in Mechanics and Materials, LDMM, Department of Mechanical Engineering, University of Djelfa, Djelfa, Algeria

ARTICLE INFO

Article history:

Received: 2024-10-09

Revised: 2025-03-27

Accepted: 2025-06-01

Keywords:

Heat exchange;
Laminar flow;
MHD;
Nano-fluid;
Wavy channel.

ABSTRACT

Simulation analysis to evaluate the impact of combined enhancement techniques on forced convection flow patterns and heat transfer is investigated in the present work. More precisely, a Newtonian nanofluidic flow flowing in complex sinusoidal geometry subjected to an external magnetic field is studied. This last is applied uniformly/non-uniformly to different values of the Hartmann number ranging from 0 to 50 in the fluid domain and oriented horizontally by; γ=0, γ= π/4 and γ=π/2. Hydrodynamic and thermal behavior changes are examined in terms of secondary flow intensity, velocity profile, shear and rotation rates, the temperature profile pattern and the non-dimensional Nusselt number. Findings illustrate that the improvement in parietal heat transfer varies depending on the applied procedure, where the percentage of increase varies from 1% to 14% depending on each case. Specifically, the full application of the magnetic field at an angle of $\pi/2$ improves the average Nusselt number from 10.5 to 12, almost by 14% compared to the no-magnetic-field scenario. Also, applying a partial magnetic field in the $\pi/4$ and $\pi/2$ orientations leads to an improvement in heat exchange of 3%, 5%, 7%, and 10% compared to the base case.

1. Introduction

Standard heat exchangers often exhibit low efficiency and high thermal resistance, necessitating advancements in design and materials. These devices facilitate heat transfer between two fluids without significant energy losses to the environment. Their operation involves fluid flow through the channels and heat exchange across the channel walls. Enhancing these processes is paramount to improving heat exchanger performance. The surface area-to-volume ratio is a fundamental factor influencing the heat transfer rate within channels, with smaller channels generally exhibiting enhanced heat transfer performance [1].

Extensive research has been dedicated to mitigating thermal resistance and augmenting heat transfer within microchannel heat exchangers (MCHXs). Steinke and Kandlikar [2] pioneered investigations into both passive and active strategies for enhancing MCHX thermal performance. While active methods, such as vibration, electric, or magnetic field manipulation, can boost heat transfer, they often require external energy input. Conversely,

*** Corresponding author.**
E-mail address: lamine_aa@yahoo.fr

Cite this article as:

Nekbil, A., Boukhalkhal, A. L., Aidaoui, L. and Lasbet, Y., 2026. Thermal Performance of CuO-Water Nanofluid Flows Within a Wavy Channel Under the Influence of an External Magnetic Field. *Journal of Heat and Mass Transfer Research*, 13(2), pp. 245-259.

https://doi.org/10.22075/jhmtr.2025.35581.1616

passive techniques, which involve modifications to channel geometry or fluid properties, offer energy-efficient improvements. These researchers conducted a thorough analysis to assess the practicality of integrating these strategies into novel MCHX applications [1].

Straight channels are commonly employed in microchannel exchangers due to their low pumping power and laminar flow conditions. However, their linear flow profile often results in inadequate mixing, leading to poor heat transfer performance. The formation of thick boundary layers along channel walls exacerbates this issue, particularly under high heat flux conditions. Additionally, these channels struggle to dissipate localized heat generated by hotspots in microelectronic devices. To address these limitations, researchers have explored various channel modifications, including incorporating grooves, ribs, waves, dimples, and fins, to induce flow instabilities and enhance mixing [3]–[6].

Ghani et al. [7] conducted a numerical study of microchannel heat sinks with rectangular ribs and secondary oblique channels. By systematically adjusting channel parameters, they identified an optimal design configuration that maximizes heat transfer while minimizing pressure drop. The optimal configuration, characterized by specific values for λ, β, and the angle, achieved an impressive performance factor of 1.98 at a Reynolds number of 500. Monavari et al. [8] investigated numerically the influence of the shape of the nanoparticle on the thermo-fluidic behavior of a MCHS featuring various cross-sections (elliptical, hexagonal, circular, and triangular). Their study revealed that a triangular microchannel heat sink exhibited superior heat transfer coefficients compared to other geometries. By examining five shapes of nanoparticles (cylinder, platelet, oblate spheroid, brick, and blade) at different Reynolds numbers, the researchers determined that platelet-shaped nanoparticles maximized heat transfer enhancement. Fadhl et al. [9] used ANFIS and GMDH to model the dynamic viscosity of MgO nanofluids, which is critical for heat transfer applications. GMDH outperformed ANFIS, showing increased accuracy with an R^2 of 0.9996 and an AARD of 5.13%. This makes it the preferred method for predicting nanofluid viscosity.

Recent studies highlight various advanced designs of MCHXs, including zigzag and serpentine channels, which improve fluid dynamics and heat transfer rates. Among these shapes, wavy channels are considered one of the most commonly used solutions to enhance heat and mass transfer.

The concept of wavy microchannels as an enhancement over traditional straight channels was pioneered by Sui et al. [6], [10], who attributed the improved heat transfer performance to Dean vortices generation. Subsequent research by Mohammed et al. [11] explored the influence of channel amplitude (125-500 μm) on wavy microchannel performance. Their findings revealed a direct correlation between microchannel amplitude and wall shear stress and friction factor. Xie et al. [12] extended this concept to wavy microchannels with double-layers, demonstrating the benefits of a counter-flow configuration. The potential of nanofluids as working fluids in wavy microchannels, investigated by Sakanova et al. [13]. Their findings demonstrated substantial enhancement in heat transfer, ranging from 5.34% to 24.1%, compared to traditional rectangular MCHSs. However, this improvement was accompanied by a notable pressure drop increase of approximately 150-421.7%. Saleem and Heidarshenas [14] numerically simulated a wavy-walled microchannel heat sink for electronic cooling applications. Employing nanofluids (water, copper oxide/water, and alumina/water), they introduced exergy analysis as a novel metric for examining the performance of heat sinks. Results indicated that nanofluids, particularly copper oxide/water, effectively reduced maximum temperature and exergy losses compared to pure water. Specifically, a 2% concentration of copper oxide or alumina lowered the maximum temperature by 2.38°C and 2.55°C, respectively, at a Reynolds number of 500. Ghorbani et al. [15] numerically investigated the thermal-hydraulic performance of wavy microchannels for electronic cooling applications. By varying channel amplitude and wavelength, they investigated the impact of these parameters on fluid flow and heat transfer. Their findings demonstrated that large amplitude-to-wavelength ratios resulted in enhanced heat transfer due to amplified secondary flows. The optimal geometry, as determined by a performance evaluation criterion, was a wavy channel with a wavelength of 2500 μm and an amplitude of 250 μm. This configuration effectively damped temperature fluctuations and prevented hotspot formation under high heat flux conditions.

Hybrid cooling systems that combine multiple approaches also show significant potential. Continued development and research in these areas is crucial to meeting the thermal management challenges posed by the next generation of microelectronic devices. Research has shown that using nanofluids in conjunction with magnetohydrodynamic (MHD) can significantly enhance heat transfer [16], [17].

Utilizing numerical simulation and machine learning, Kumar et al. [18]–[21] presented studies advancing heat transfer and fluid dynamics. Their work demonstrates proficiency in applying computational and machine learning methodologies to analyze and optimize fluid flow and heat transfer in intricate nanofluid and magnetic field systems. This work targets applications from thermal management to coating technologies.

Hamzah et al. [22] conducted a numerical analysis of nanofluid natural convection in a wavy porous enclosure subjected to a magnetic field, utilizing a validated computational model. Their findings indicate that: the magnetic field exhibits limited influence at high Rayleigh (Ra) and low Darcy (Da) numbers; thermal conduction is enhanced at high Hartmann (Ha) and low Rayleigh (Ra) numbers; surface waviness and Darcy (Da) number significantly impact heat transfer suppression; and, at Ra = 10^5, nanoparticle volume concentration reduces the mean Nusselt number, especially at high Ha.

Through a series of studies using numerical and statistical methods, Shah et al. explored diverse heat transfer and fluid dynamics problems involving nanofluids and hybrid nanofluids. These investigations covered: ternary hybrid nanoparticles in pseudo-plastic fluids [23]; squeezed nanofluid flow over magnetized sensors [24]; water-based hybrid nanofluids in porous media [25]; and micropolar bioconvection nanofluids over Riga plates [26], showcasing their expertise in applying computational techniques to optimize heat transfer.

Numerical investigations have focused on optimizing the MHD effect in microchannel configurations. Cho et al. [27] conducted a numerical study to investigate the influence of inclination angle, nanoparticle concentration, Rayleigh number, and wavelength amplitude on heat transfer and entropy generation in an Al2O3-water nanofluid-filled enclosure. Their findings revealed that inclination angle significantly impacted heat transfer, flow parameters, and entropy generation, particularly at elevated Reynolds numbers. Higher nanoparticle concentration correlated with increased Nusselt number and decreased entropy generation. Moreover, wavy surfaces demonstrated superior heat transfer performance to regular surfaces while concurrently reducing total entropy generation. Mamourian et al. [28] employed the Taguchi method to minimize entropy generation and optimize heat transfer in a wavy enclosure containing a copper-water nanofluid. By considering parameters such as a wavy surface wavelength, nanoparticle volume fraction, and Richardson number, they identified optimal conditions for a heat exchanger design. Their findings revealed a trade-off between entropy generation and heat transfer enhancement, with larger wavelengths generally leading to decreased heat transfer and entropy production. The optimal configuration was determined to be a volume fraction of 2%, a wavelength of 0.25, and a Richardson number of 0.001. Asadi et al. [29] explored the influence of nanoparticle concentration, Reynolds number, wavy channel amplitude, and negative magnetic field gradient on the thermal performance and hydrodynamic properties of a ferrofluid within a microchannel. Their findings indicated that increasing these parameters generally led to enhanced heat transfer, as evidenced by the Nusselt number. However, the application of a negative magnetic field gradient, while improving heat transfer, also resulted in increased pump work, especially at lower Reynolds numbers.

The work conducted by Aidaoui et al. [30], [31] provided valuable insights into the synergistic effects of chaotic flow, nanofluids, and magnetic fields on heat transfer enhancement. Results indicated a significant increase in the Nusselt number, particularly for partial magnetic field applications in the perpendicular direction. The study highlighted the potential of this combined approach for improving heat transfer efficiency, with a potential improvement of up to 13%, versus the initial case. Recently, Kenniche et al. [32] conducted a numerical investigation into enhancing thermal mixing and fluid dynamics in three-dimensional open flow channels using an external magnetic field (MHD). By employing complex geometry, nanofluids, and non-uniform magnetic fields, the study aimed to optimize mixing efficiency and heat transfer. The results indicated that a non-uniform magnetic field oriented at $\pi/2$ or $\pi/4$ degrees yielded the most significant improvements in mixing degrees, exceeding 90%. Additionally, the Nusselt number increased by over 45% under optimal conditions.

In contrast to the abundant literature on the uniform magnetohydrodynamic (MHD) effects of nanofluids on hydrothermal characteristics, studies on non-uniform MHD are severely restricted. Moreover, while some research exists on non-uniform MHD in various geometries, the impact on wavy channels remains entirely unexplored. This study numerically analyzes the hydrothermal properties of nanofluids within a wavy channel, considering the effects of both uniform and non-uniform magnetohydrodynamic (MHD) fields.

The non-uniform magnetohydrodynamic field will be applied to the wavy channel in two ways: firstly, a full application of MHD to the entire wavy channel, and secondly, a partial application

of MHD. By employing a combination of active and passive methods simultaneously with a non-uniform MHD field, the study significantly enhances the partial heat transfer performance compared to scenarios with no magnetic field and fully applied magnetic field at all. In consequence, in this study, a numerical assessment is conducted to assess the thermal performance improvement of copper-oxide-water nanofluid flows within a wavy channel under the influence of an external magnetic field. Specifically, the impact of magnetic field orientation (0°, π/4, π/2) and Hartmann number (0~50) on hydrodynamic and thermal behavior is systematically explored.

2. Problem Description

This study investigates the flow of CuO-water nanofluid through a two-dimensional wavy channel. Figure 1 depicts the channel geometry characterized by four identical annuli with a rotation angle ϕ and an axial width S. The full wavy channel is formed by five periods. The dimensionless parameters α = S/L and ϕ represent the channel's axial width and rotation angle, respectively. For this study, α was set to 0.1, and ϕ was set to π/4.

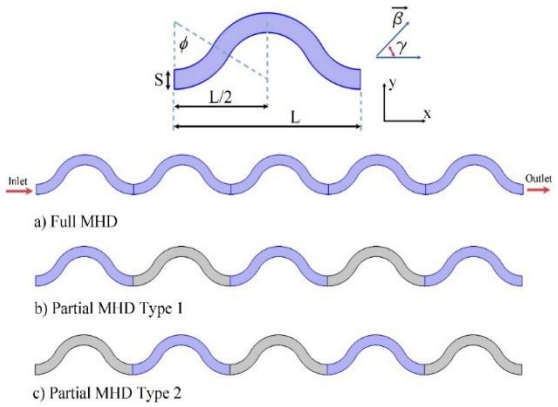

Fig. 1. The considered wavy channel

A constant heat flux of 10,000 W/m² was applied to the entire outer wall of the channel, while a temperature T_c and uniform inlet velocity u_0 were prescribed at the wavy channel entrance.

The numerical simulations assume a two-dimensional, steady, incompressible, and Newtonian nanofluid flow within the channel. To investigate the influence of the orientation of a magnetic fields, three scenarios were considered: a magnetic field applied across the entire five-wave channel length, and two partial application scenarios, depicted in figures 1b and 1c. Table 1 presents pure water and copper-oxide nanoparticles' thermophysical properties under the assumption of thermal equilibrium.

Table 1. Copper-oxide nanoparticles and pure water thermophysical properties

Property	CuO Nanoparticles	Pure Water
Cp	383	4179
ρ	8954	997.1
k	400	0.6
μ	/	1003 10-6
β	1.67 10-5	2.1 10-4
σ	5.96 107	0.05

3. Mathematical Formulation

The continuity, energy, and momentum governing equations of the nanofluid flow were considered under steady-state conditions in this study. The fluid was modeled as an incompressible Newtonian fluid.

$$\frac{\partial u}{\partial x}+\frac{\partial v}{\partial y}=0 \tag{1}$$

$$u\frac{\partial u}{\partial x}+v\frac{\partial u}{\partial y}=-\frac{1}{\rho_{nf}}\frac{\partial P}{\partial x}+\nu_{nf}\left(\frac{\partial^2 u}{\partial x^2}+\frac{\partial^2 u}{\partial y^2}\right)+\frac{\sigma_{nf}B_0^2}{\rho_{nf}}(v(sin(\gamma)\cos(\gamma))-u(\sin(\gamma))^2) \tag{2}$$

$$u\frac{\partial v}{\partial x}+v\frac{\partial v}{\partial y}=-\frac{1}{\rho_{nf}}\frac{\partial P}{\partial y}+\nu_{nf}\left(\frac{\partial^2 v}{\partial x^2}+\frac{\partial^2 v}{\partial y^2}\right)+\frac{\sigma_{nf}B_0^2}{\rho_{nf}}(u(sin(\gamma)\cos(\gamma))-v(\cos(\gamma))^2) \tag{3}$$

$$u\frac{\partial T}{\partial x}+v\frac{\partial T}{\partial y}=\alpha_{nf}\left(\frac{\partial^2 T}{\partial x^2}+\frac{\partial^2 T}{\partial y^2}\right) \tag{4}$$

α_{nf} indicates the thermal diffusivity of the Copper-Oxide-water, which is equal to $\frac{K_{nf}}{\rho_{nf}Cp_{nf}}$.

The energy equation for this study neglected the effects of Joule heating and viscous dissipation.

The following equations presented the thermophysical characteristics of the nanofluid, including thermal expansion coefficient, density, specific heat, and electrical conductivity [33]:

$$\rho_{nf}=(1-\emptyset)(\rho_f)+\emptyset\rho_s \tag{5}$$

$$(\rho C_p)_{nf}=(1-\emptyset)(\rho C_p)_f+\emptyset(\rho C_p)_s \tag{6}$$

$$\sigma_{nf}=(1-\emptyset)(\sigma_f)+\emptyset\sigma_s \tag{7}$$

$$(\rho\beta)_{nf}=(1-\emptyset)(\rho\beta)_f+\emptyset(\rho\beta)_s \tag{8}$$

The lowercase letters nf, s, and f refer to nanofluid, solid particle, and the base fluid respectively, while ∅ denotes the volume fraction of solid particles.

Following Brinkman [34], nanofluid dynamic viscosity can be expressed as follows:

$$\mu_{nf} = \mu_f (1 - \emptyset)^{-2.5} \tag{9}$$

By using the Maxwell-Garnett model [35], the copper-oxide-water nanofluid thermal conductivity is:

$$k_{nf} = k_f \frac{(k_s + 2k_f) - 2\emptyset(k_f - k_s)}{(k_s + 2k_f) - \emptyset(k_f - k_s)} \tag{10}$$

The effective electrical conductivity of the CuO-water nanofluid was determined using Maxwell's model [35]:

$$\sigma_{nf} = \sigma_f (1 + \frac{3\left(\frac{\sigma_s}{\sigma_f} - 1\right)\emptyset}{\left(\frac{\sigma_s}{\sigma_f} + 1\right) - \left(\frac{\sigma_s}{\sigma_f} - 1\right)\emptyset} \tag{11}$$

The governing equations were non-dimensionalized using the following dimensionless parameters:

$$U = \frac{u}{u_0}, V = \frac{v}{u_0}, X = \frac{x}{D_h}, Y = \frac{y}{D_h},$$

$$P = \frac{p}{\rho_f {u_0}^2}, \theta = \frac{T - T_c}{\Delta T}, \Delta T = \frac{q\, D_h}{k_f}, \tag{12}$$

$$Pr = \frac{\mu_f\, Cp_f}{k_f}, Re = \frac{u_0\, D_h}{\nu_f}, Ha = B_0\, D_h \sqrt{\frac{\sigma_f}{\nu_f}}$$

4. Simulation Protocol

The governing equations are solved using the Galerkin weighted residual element formulation with the suitable boundary conditions mentioned above. This formulation establishes the weakest version of the governing equations and sets the weighted average residuals of the approximated flow field variables to zero. The weight function is chosen from the same set of functions as ones of the trial functions. Triangular elements were employed for computational domain discretization. Triangular Lagrange finite elements of various orders are used to approximate all variables in the discretized computation domain. Commercial computational fluid dynamics (CFD) solver Comsol was used in this study. Convergence was achieved when the relative error of all variables reached 10^{-6}.

5. Validation

To validate the accuracy of the CFD code configuration, a comparative study was conducted with the work of Pirmohammadi and Ghassemi [36] (see figure 2). The computed isotherms and streamlines for various Hartmann and Rayleigh number values were demonstrated high consistency with their results, confirming the reliability of the code for simulating the present heat and fluid flow phenomena.

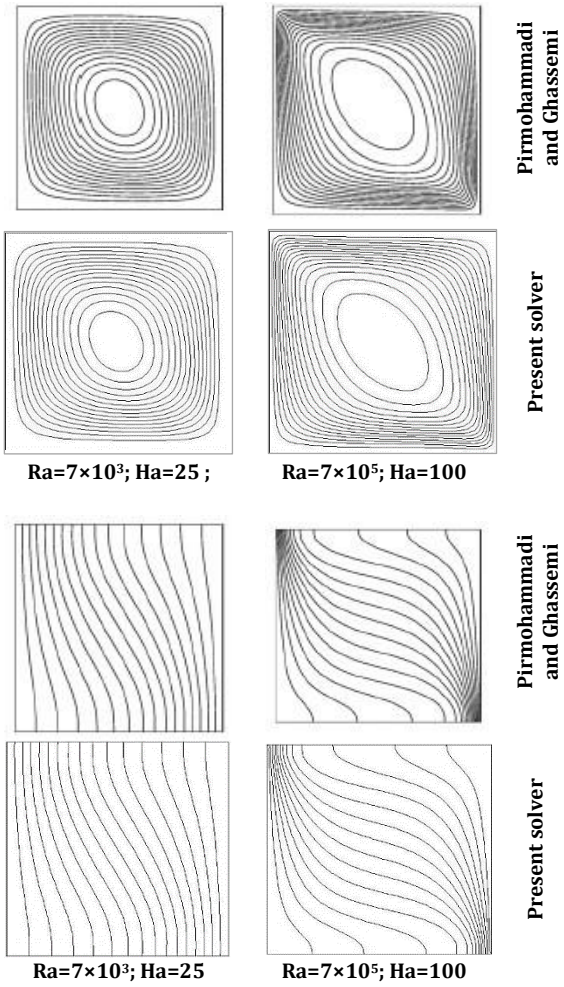

Fig. 2. Validation of the current solver against the work of reference [36]

To further validate the numerical solver, a comparative study was conducted on the findings of Selimefendigil and Oztop [37]. The study examined a nanofluid-filled cavity containing a rotating central cylinder within a magnetic field. By comparing the predicted local Nusselt number values for specific conditions (Ω = 0, Ha = 20, ϕ = 0.02) with the reference data, excellent agreement was observed, where the percentage deviation between the current solution data and the reference 37 is equal to 5.9% confirming the solver's accuracy and reliability (see figure 3).

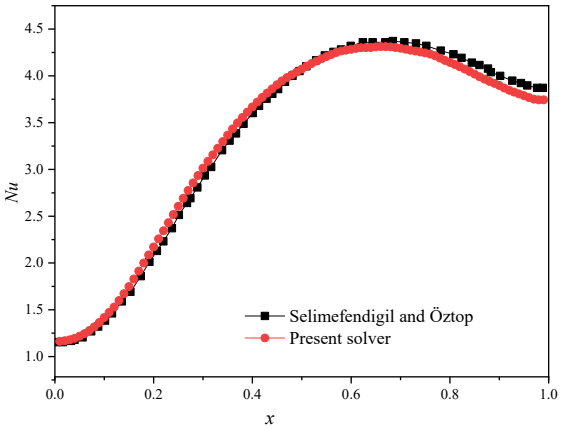

Fig. 3. Validation of the local Nusselt number evolution with reference to [37]

6. Grid Study

To achieve accurate results in this CFD study, a mesh independence test was performed. Four grid sizes of 6000, 13500, 24000, and 37500 elements were examined using a structured triangular grid. To determine the optimal grid, axial velocity profiles at x = 12.5 cm along the y direction were compared across four grids (figure 4). The near-identical profiles of Grid 3 and Grid 4 confirmed that Grid 3 provided sufficient accuracy, making it the selected grid for further simulations.

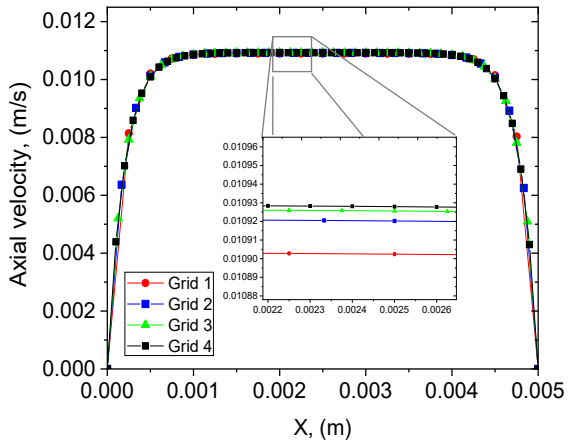

Fig. 4. Axial velocity variation in y direction for various grid sizes

7. Results and Discussion

The current project aims to find the appropriate protocol to help the enhancement of the mechanical and energetic performance of laminar forced convection flow in a wavy geometry. Hydrodynamic and thermal comportments of the considered flow in the presence of an external magnetic force are presented under various parameters such as velocity field, shear and rotation rates, parietal heat exchange and temperature field.

7.1. Hydrodynamic Comportment

a. Shear and rotation rates

It is well known that mixing procedures are strongly influenced by shearing and elongation processes. The strain tensor's non-diagonal component, shear, aids in dispersing droplets inserted into immiscible fluid flow. Stretching and folding the volume elements in the direction of flow is facilitated by elongation, the diagonal part of the deformation tensor. Moreover, flow rotation improves mass and heat mixing by generating flows in transverse directions.

The average values of shear rate and rotation rate along with the magnetic field strength presented in terms of Hartmann number are illustrated respectively in figures 5 and 6. Examination is performed for various inclination angles of magnetic force at 0, $\pi/4$ and $\pi/2$ with fixed Reynolds number equal to 100. Two manners of applying external magnetic force are considered, either to the entire geometry called full-MHD or to selected parts of the geometry named partial-MHD. Also partial MHD is applied in two types; first to three portions of five, then two portions of five as shown in figure 1.

In figure 5 (upper panel) the fluctuation of the shear rate as a function of Hartmann number ranging between 0 and 50 is presented at a fixed value of Re = 100. The effect of the magnetic force mode (full or partial) on the shear rate evolution is appeared for the three considered angles of orientation (0, π /4 and π /2). While the lower panel of figure 5 illustrates the evolution of the shear rate with Hartmann number and the effect of orientation angle in each manner of applying the magnetic field (full, the two types of partial modes). It is noted that the shear rate variation is either decreased or maintained constant except when applying the full MHD mode with an orientation angle of 0 where it decreased first and then increased from the value Ha = 20. This value appears critical where the fluid changes its hydrodynamic behavior.

We have shown that the velocity field is significantly affected by magnetic fields, especially according to a well-defined protocol. This modification of the dynamic field leads to a re-evaluation of the local behavior of the flow, presented by strain rate, rotation rate, trajectories, etc. This fact is confirmed, because the strain and rotation tensors are directly related to the velocity gradient tensor.

In figure 6, the rotation rate variation with Hartmann number with Re=100 is shown for various modes of MHD field in the three orientation angle cases (upper panel). Rotational motion is very important in fluids in order to achieve the fluid mixing process quickly. The

rotation rate maintains the same evolution as the shear rate with a minimum value at a Hartmann number equal to 20. In the lower panel the rotation rate evolution is presented along with the Hartmann number for the considered orientations of the magnetic force and in the case of the examined modes of the magnetic field, full/partial. As a general overview, the orientation rate value is always decreased or maintained constant in all the proposed cases of magnetic mode and orientation by increasing the Hartmann number.

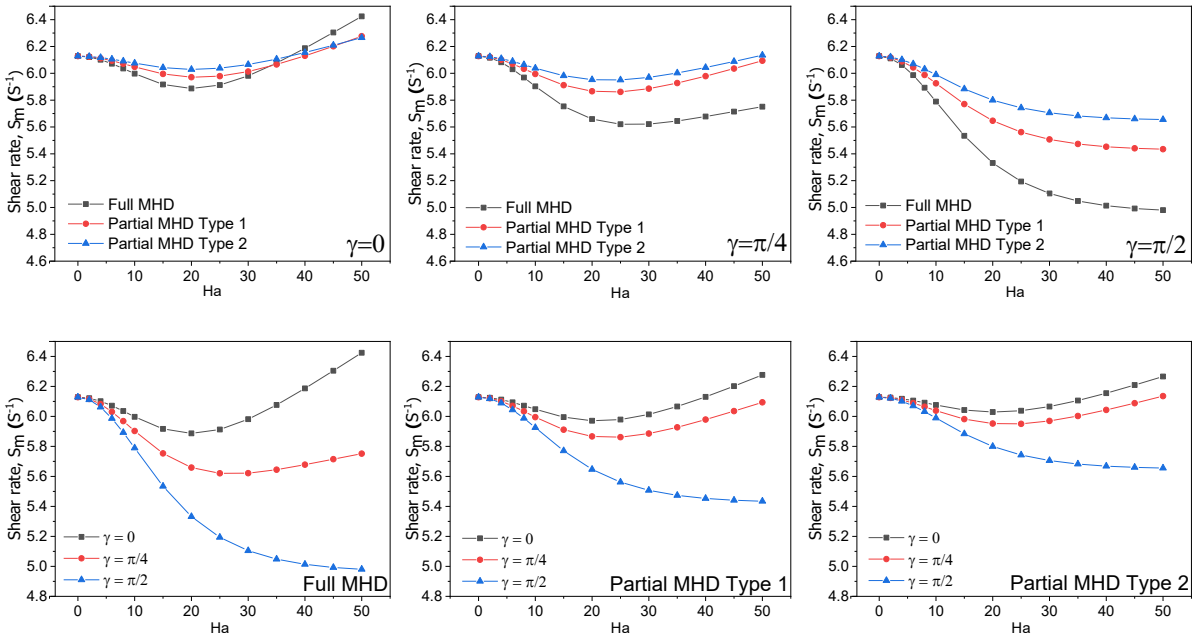

Fig. 5. Shear rate Sm evolution with Hartmann number Ha by applying the MHD in partial and full modes for Re=100

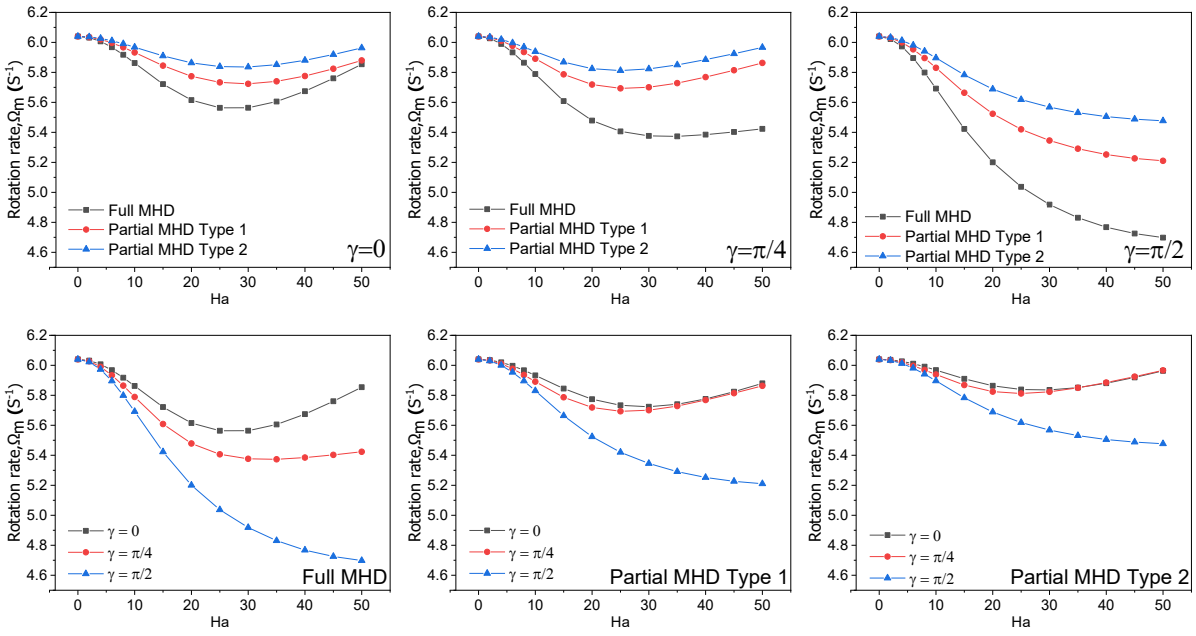

Fig. 6. Rotation rate Ωm evolution with Hartmann number Ha by applying the MHD in partial and full modes for Re=100

b. Intensity of secondary flow

The intensification of transfer phenomena such as mixing and parietal heat exchange depends closely on fluid residence time increase. For this purpose, secondary flows are created by applying a magnetic field according to a well-defined protocol.

This leads to the creation of mixers that prevent dead zones from forming in the flow by breaking the flow regularity. The following is a presentation of the intensity equation.

$$I = \frac{\bar{V}_y}{|V|} \tag{13}$$

Figure 7 shows the fluctuations of the intensity feature along with Ha number ranging between 0 and 50 for Re=100, with an MHD field applied in three different manners, partial 1, partial 2, and complete, oriented in the directions; $\gamma = 0$, $\gamma = \pi/4$ and $\gamma = \pi/2$. For the three considered modes of the external magnetic field (full, partial 1 and 2), the intensity decreases when the orientation angle is equal to 0. Moreover, a slight augmentation of the intensity is observed when the MHD force is oriented at an angle $\gamma = \pi/4$ whatever the MHD mode. This can be explained by the fact that the magnetic force work is increased when the angle $\gamma = \pi/4$. Besides, heat transfer is directly impacted by the intensification of secondary flows.

c. Velocity profile

The angle between the magnetic force and the fluid displacement in the channel is of paramount importance, as it determines the amount of work done by magnetic force. Therefore, we propose three main orientations: 0, $\pi/4$, and $\pi/2$.

The synergy between the value of Ha, orientation angle (γ) and the mode of application (Full or Partial) of the magnetic field considerably affects dynamic field behavior. In other words, the velocity field profile becomes more complex when an appropriate protocol is applied to the flow domain.

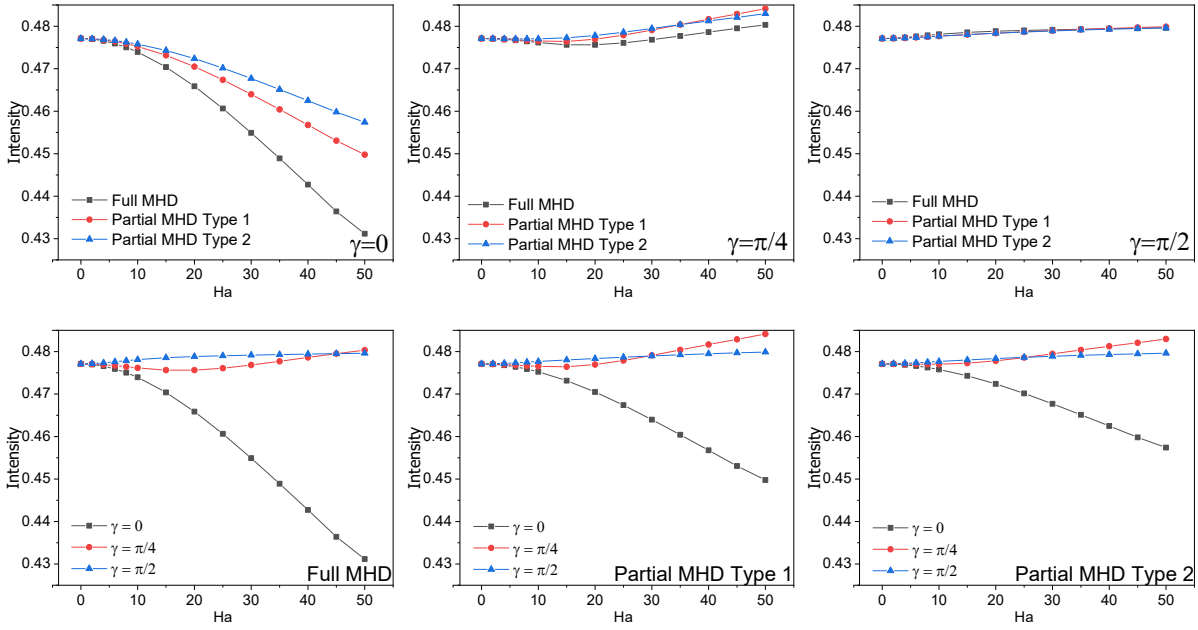

Fig. 7. Intensity evolution with Hartmann number Ha by applying the MHD in partial/full modes for Re=100

The axial velocity profile drawn in the y direction at x=0.15 m is shown in figures 8 and 9. Simulated profiles are presented for different values of Hartmann number ranging between 0 and 50. They are presented under the effect of the three magnetic field modes, full and partial oriented by the angles 0, $\pi/4$ and $\pi/2$. The considered Reynolds number during these computations is constant and equal to 100.

For an orientation angle of the magnetic field $\gamma=0$, the velocity profile shapes have a parabolic form with a maximum value at the section center whatever the applied MHD mode. This form was kept until a value of Hartmann Ha = 20 where it started moving towards the channel wall recording an augmentation in its maximum values.

The maximum velocity shifts sometimes towards the upper wall and sometimes towards the lower wall. This oscillation provides an excellent opportunity for better wall heat transfer. Based on this result, we can combine different protocols on the same pipeline. When the orientation angle is fixed at $\gamma= \pi/2$, for all the studied magnetic modes and with increasing the Hartmann number the axial velocity profiles become more flat with a decrease in the center.

Moreover, an acceleration of fluid flow is observed near the duct wall which leads to improving parietal heat transfer. Also, close to the wall, a significant velocity gradient is created, which raises the strain rate. In the case of $\gamma= \pi/4$ a mixture of the previous two patterns is observed depending on the magnetic field mode (full, partial 1 or 2).

The protocol type can influence the flow regime. If the fluid is decelerated, the transition from laminar to turbulent is delayed. On the other hand, if the fluid is accelerated, the transition point occurs at a Reynolds number higher than the standard value.

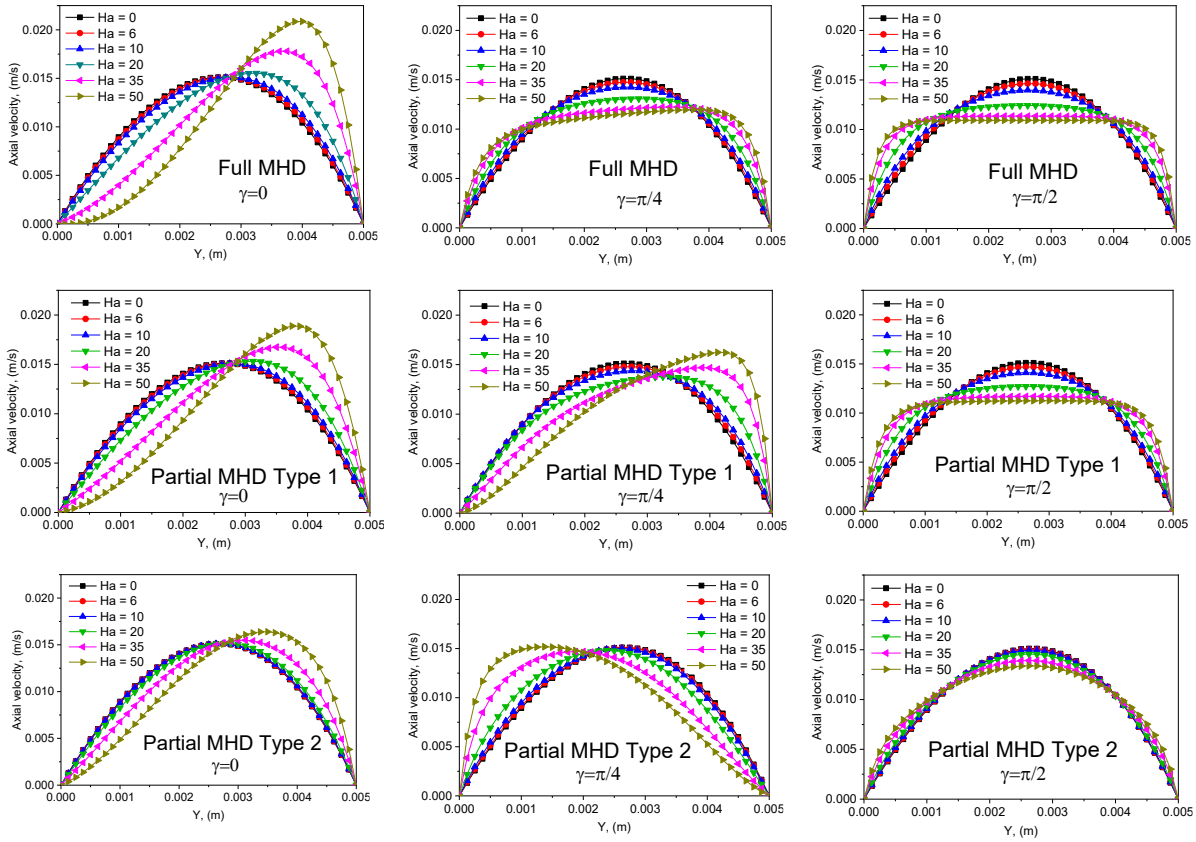

Fig. 8. Variation of axial velocity profiles along Y coordinate at x = 0.15m for various Ha values, by applying the MHD in partial and full modes for Re=100

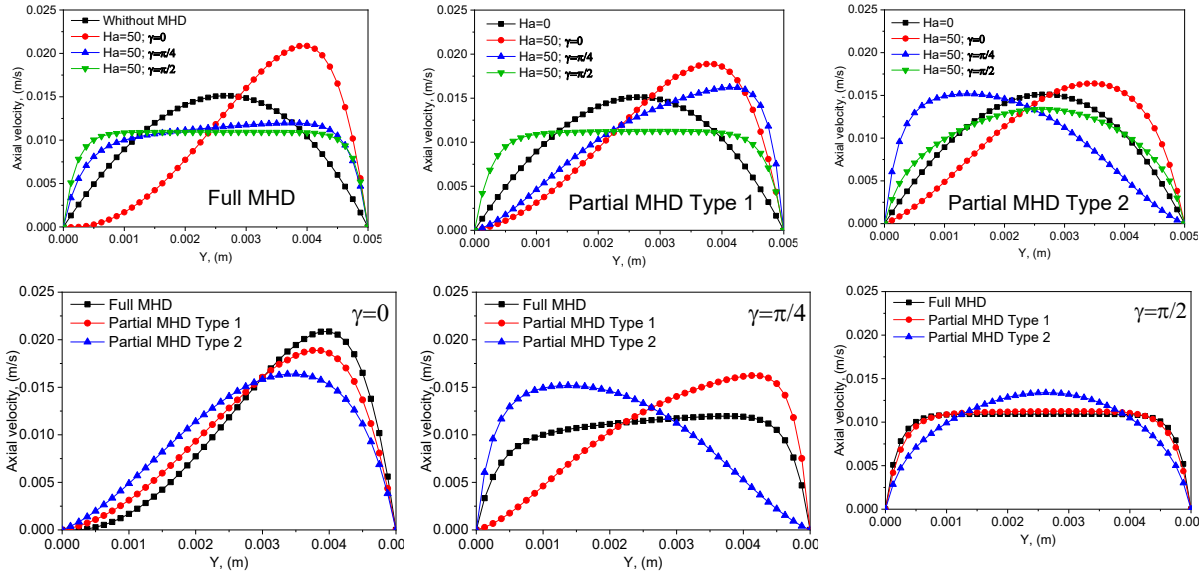

Fig. 9. Variation of axial velocity profiles along Y coordinate at x = 0.15m by applying the MHD in partial and full modes, for Ha = 50 and Re=100

7.2. Thermal Comportment

As known, in the fluid domain the velocity field transports the temperature, which is an inactive scalar. In order to assess the impacts of applying the MHD field in various modes and intensities, the thermal field will be examined with temperature profiles and the dimensionless number of Nusselt.

a. Temperature profile

Figure 10 indicates the evolution of temperature profiles with Y coordinate at a fixed point x= 0.15m. The examination is carried out for three values of the Hartmann number 0, 10 and 50. The imposed MHD fields are applied in two methods, complete and partial and oriented to 0, π/4 and π/2.

It has been noted that when the MHD force is oriented by γ= π/2, profiles of temperature become more uniform. The disparity between the maximum and minimum values is lessened mainly in full and partial modes. As a result, the temperature reaches its maximum value near the domain boundaries. Indeed, the flow creates secondary flow that move the fluid transversely. While in the case of γ=0 with a fully or partially applied magnetic field, the parabolic form of the temperature profile is lost and its maximum value approaches the channel wall.

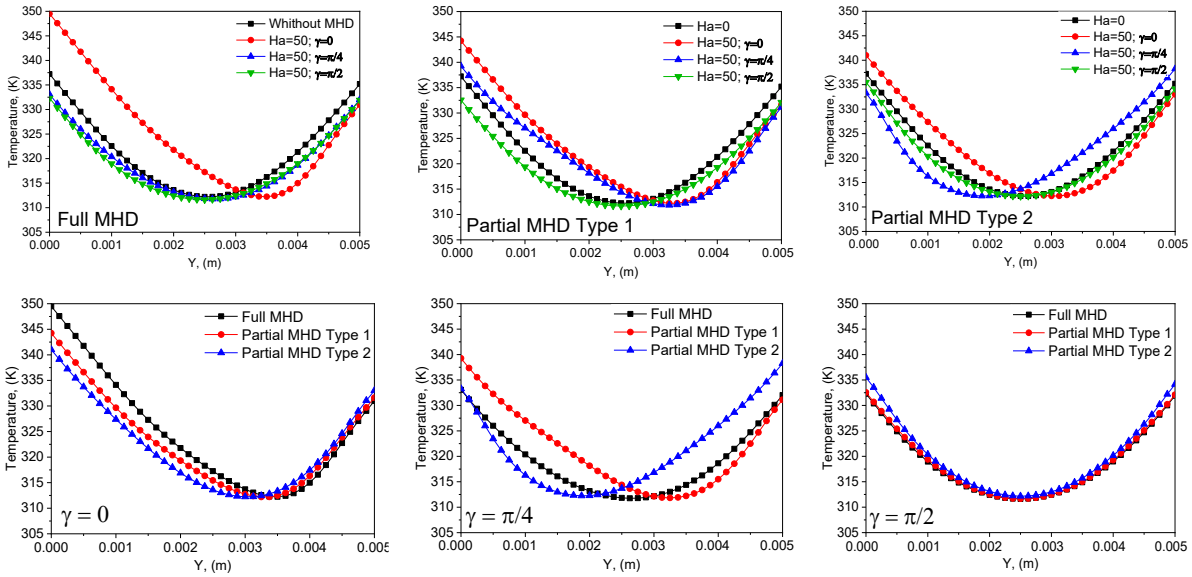

Fig. 10. Variation of temperature profiles along Y coordinate at x =0.15m with full/partial magnetic modes and various orientations with Re=100 for the lower panel Ha=50

b. Heat transfer

The dimensionless quantity adopted to study parietal heat exchange is the Nusselt number, as defined by equations 14 and 15:

$$Nu_l = \frac{qD_h}{k\,(T_w - T_m)} \tag{14}$$

$$Nu_m = \frac{1}{L}\int_0^L Nu_L dA \tag{15}$$

T_w and T_m represent wall and bulk mean temperatures, respectively. Nu_m and Nu_L denote the average and local Nusselt numbers, respectively.

Figures 11 and 12 demonstrate the progress of the mean Nusselt number with Hartmann number ranging between 0 and 50 and for a fixed value of Reynolds number equal to 100. The average Nusselt values are analyzed for different protocols presented in terms of types of external magnetic field application (full, partial) oriented to 0, $\pi/4$ and $\pi/2$. Findings proved that the mentioned protocols of applying the external magnetic field to the fluid flows in a complex geometry always improve heat transfer. Depending on the applied procedure, the parietal heat transfer enhancement can range from 1% to 14%. More precisely, the full use of the magnetic field directed by an angle equal to $\pi/2$ enhances the mean Nusselt value from 10.5 to 12 at Ha=50 by almost 14% compared to the case without a magnetic field.

By using this method, the fluid near the wall can be accelerated, which reduces the amount of dynamic and thermal boundary layers which posing obstacles to a better transmission of momentum and heat. Other combined techniques with applying partial magnetic fields in $\pi/4$ and $\pi/2$ orientation also lead to heat exchange improvement with different ratios; 3%, 5%, 7% and 10% by comparison with the base case where no magnetic field is applied.

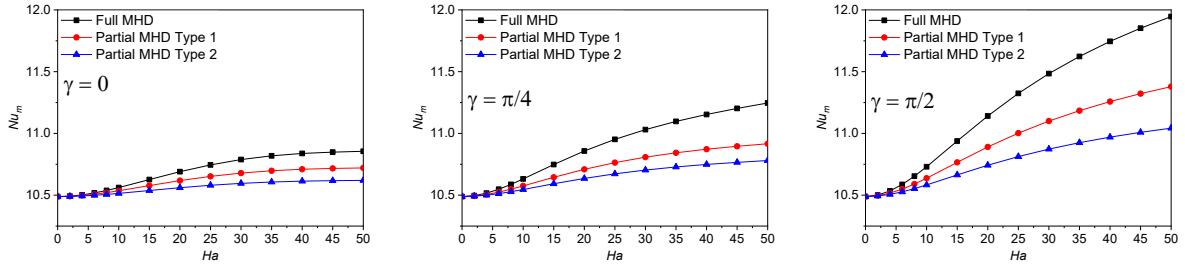

Fig. 11. Mean Nusselt number evolution along Ha with full/partial MHD modes for Re=100

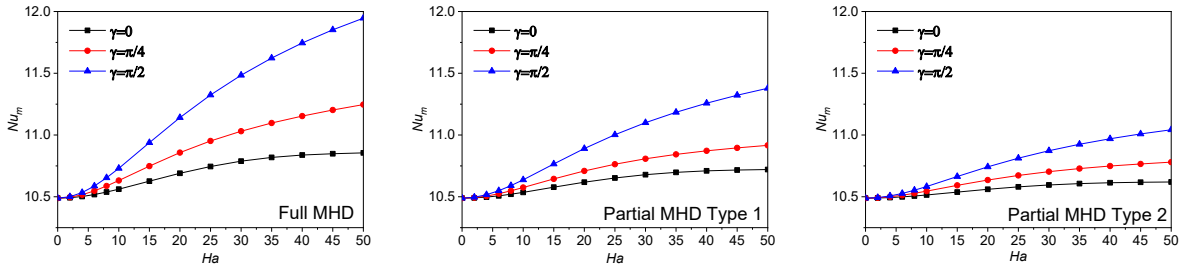

Fig. 12. Mean Nusselt number evolution along Ha, three angles of the magnetic field applied in full/partial modes with Re=100

As mentioned before, the heat transfer between the hot wall and the fluid is distinguished by the Nusselt number, which is directly related to the fluid's flow characteristics.

Figure 13 displays how the Hartmann number impacts local Nusselt number evolution at selected cross sections following the x direction while taking into account various modes and magnetic field orientations.

The evolution of the local Nusselt number shows the fluctuating behavior of this quantity along the mean line of the channel. This behavior is explained by the rupture of the dynamic and thermal boundary layers due to the complexity of the geometry and the presence of the partial magnetic field, in particular at large values of the Hartmann number. Due to the large temperature differential between the lateral surface and the nanofluid flow in the inlet section, the local Nusselt number Nul exhibits maximal values at the channel entrance in all examined cases. Once the flux is fully developed, it generally remains constant, with the lowest values observed at the outlet, whether the magnetic field is fully applied or not.

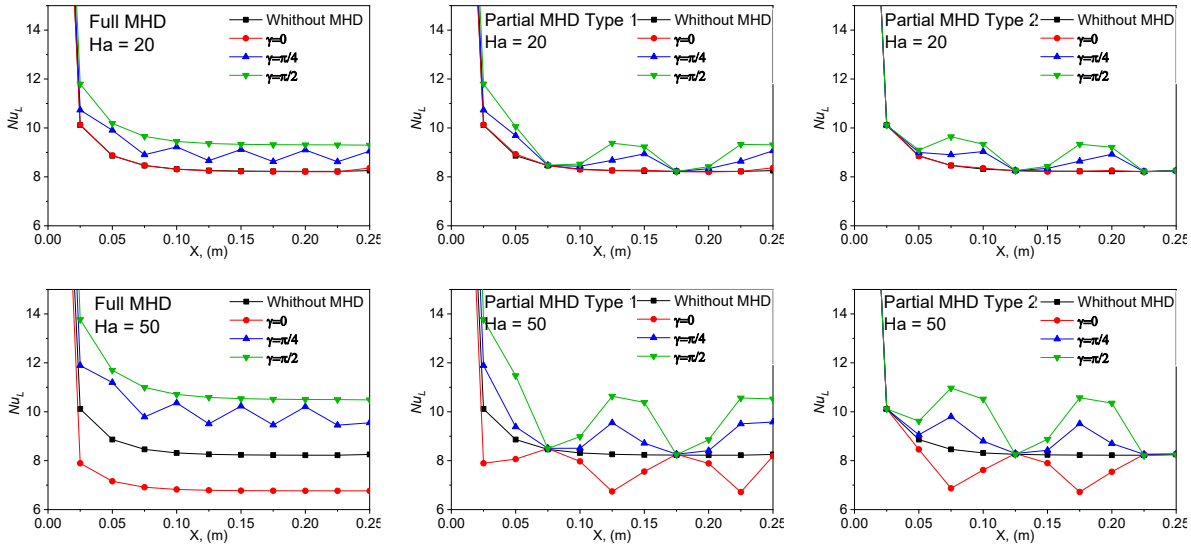

Fig. 13. Local Nusselt number evolution at selected cross sections following the x direction for Re = 100, two values of Ha (20, 50), and various orientations of the magnetic field applied with full/partial modes

8. Conclusions

In the present project, a 2D numerical study is conducted to evaluate the effect of combined enhancement methods on the local physical properties and thermal behavior of an open forced convection flow. Specifically, a Newtonian nanofluidic flow flowing in a sinusoidal geometry subjected to a non-uniform external magnetic field is studied. In addition to the passive techniques presented in terms of nanoparticles added to the base fluid and wavy geometry, a magnetic field is applied non-uniformly for different values of the Hartmann number ranging from 0 to 50 in the fluid domain and oriented against the horizontal by; $\gamma=0$, $\gamma=\pi/4$ and $\gamma=\pi/2$. The changes in hydrodynamic behavior of the flow of interest are examined in terms of velocity profile, shear and rotation rates, as well as the secondary flow intensity. Furthermore, the impact of the proposed improvement protocols on thermal comportment is analyzed by evaluating the temperature profile pattern and changes in the non-dimensional Nusselt number. After examination, the findings allowed us to draw some conclusions to help in the selection of optimal cases. The improvement of wall heat transfer varies depending on the applied procedure, where the percentage increase varies from 1% to 14% depending on each case. It is

estimated that utilizing hybrid nanofluids will increase heat transfer by approximately 5% in minichannel forced convection [38]. The full application of the magnetic field at $\pi/2$ with the horizontal significantly improves the average Nusselt number from 10.5 to 12 at Ha=50 by almost 14%. Using this combination, the fluid near the wall can be accelerated, which reduces the amount of thermal and dynamic boundary layers, the last constituting obstacles to a best transfer of momentum and heat. Combining a partial magnetic field with orientations $\pi/4$ and $\pi/2$ also improves heat exchange by 3%, 5%, 7% and 10% compared to the base case without a partial magnetic field. This improvement is of great importance for being able to invest in stationary industrial applications containing cooling processes, namely hydrogen fuel cells, batteries, etc.

Nomenclature

B_0 intensity of a magnetic field
Cp specific heat (J /kg K)
D_h hydraulic diameter (m)
g gravity (m/s^2)
Ha Hartmann number
I Intensity
k thermal conductivity (W/m K)
Nu Nusselt number
p pressure (Pa)
P dimensionless pressure
q heat flux density (W/m^2)
Ra Rayleigh number
Re Reynolds number
S_m shear rate (s^{-1})
T temperature (K)
u, v x and y directional velocities (m/s)
U, V dimensionless velocities
x, y Cartesian coordinates (m)
X, Y dimensionless coordinates

Abbreviations

Al_2O_3 Aluminum oxide
Cu Copper
CuO Copper oxide
CFD computational fluid dynamics
MCHS Microchannel heat sink
MCHX Microchannel heat exchanger
MHD Magnetohydrodynamic

Greek characters

α thermal diffusivity (m^2/s)
θ dimensionless temperature
β thermal expansion coefficient (1/K)
γ magnetic inclination angle (radians)
ν kinematic viscosity (m^2/s)
σ electrical conductivity (1/Ω.m)
ρ fluid density (kg /m^3)
μ dynamic viscosity (Pa.s)
ϕ solid volume fraction (%)
Ω_m rotation rate (1/s)

Subscripts

c cold
f fluid
l local
m average
nf nanofluid
s solid
w wall

Acknowledgments

This research was supported by the directorate general DGRSDT under the authority of the Algerian Ministry of high education and scientific research.

Funding Statement

This research did not receive any specific grant from funding agencies in the public, commercial, or not-for-profit sectors.

Conflicts of Interest

The author declares that there is no conflict of interest regarding the publication of this article.

Authors Contribution Statement

Amar Nekbil: Data Curation; Formal Analysis; Validation; Visualization; Roles/Writing – Original Draft.

Ahmed Lamine Boukhalkhal: Conceptualization; Methodology; Project administration; Resources; Supervision; Writing – Review & Editing.

Lakhdar Aidaoui: Conceptualization; Methodology; Project administration; Resources; Supervision; Writing – Review & Editing.

Yahia Lasbet: Project administration.

References

[1] Dwivedi, A., Khan, M. M., Pali, H. S., 2023. A comprehensive review of thermal enhancement techniques in microchannel heat exchangers and heat sinks. J. Therm. Anal. Calorim, 148(23), pp. 13189–13231. doi: 10.1007/S10973-023-12451-3.

[2] Steinke, M. E. and Kandlikar, S. G., 2006. Single-phase liquid friction factors in microchannels. Int. J. Therm. Sci., 45(11), pp. 1073–1083. doi: 10.1016/j.ijthermalsci.2006.01.016.

[3] Chiam, Z. L., Lee, P. S., Singh, P. K., Mou, N., 2016. Investigation of fluid flow and heat transfer in wavy micro-channels with alternating secondary branches. Int. J. Heat Mass Transf., 101, pp. 1316–1330. doi: 10.1016/j.ijheatmasstransfer.2016.05.097.

[4] Sakanova, A., Keian, C. C., Zhao, J., 2015. Performance improvements of microchannel heat sink using wavy channel and nanofluids. Int. J. Heat Mass Transf., 89, pp. 59–74. doi: 10.1016/j.ijheatmasstransfer.2015.05.033.

[5] Mohammed, H. A., Bhaskaran, G., Shuaib, N. H., Abu-Mulaweh, H. I., 2011. Influence of nanofluids on parallel flow square microchannel heat exchanger performance. Int. Commun. Heat Mass Transf., 38(1), pp. 1–9. doi: 10.1016/j.icheatmasstransfer.2010.09.007.

[6] Sui, Y., Lee, P. S., Teo, C. J., 2011. An experimental study of flow friction and heat transfer in wavy microchannels with rectangular cross section. Int. J. Therm. Sci., 50(12), pp. 2473–2482. doi: 10.1016/j.ijthermalsci.2011.06.017.

[7] Ghani, I. A., Sidik, N. A. C., Mamat, R., Najafi, G., Ken, T. L., Asako, Y., Japar, W. M. A. A., 2017. Heat transfer enhancement in microchannel heat sink using hybrid technique of ribs and secondary channels. Int. J. Heat Mass Transf., 114, pp. 640–655. doi: 10.1016/j.ijheatmasstransfer.2017.06.103.

[8] Monavari, A., Jamaati, J., Bahiraei, M., 2021. Thermohydraulic performance of a nanofluid in a microchannel heat sink: Use of different microchannels for change in process intensity. J. Taiwan Inst. Chem. Eng., 125, pp. 1–14. doi: 10.1016/j.jtice.2021.05.045.

[9] Fadhl, B. M., Makhdoum, B. M., Ma'arif, A., Suwarno, I., Hamzah, H., Salem, M., 2023. Dynamic viscosity modeling of nanofluids with MgO nanoparticles by utilizing intelligent methods. Energy Reports, 9, pp. 5397–5403. doi: 10.1016/j.egyr.2023.04.369.

[10] Sui, Y., Teo, C. J., Lee, P. S., Chew, Y. T., Shu, C., 2010. Fluid flow and heat transfer in wavy microchannels. Int. J. Heat Mass Transf., 53(13), pp. 2760–2772. doi: 10.1016/j.ijheatmasstransfer.2010.02.022.

[11] Mohammed, H. A., Gunnasegaran, P., Shuaib, N. H., 2011. Numerical simulation of heat transfer enhancement in wavy microchannel heat sink. Int. Commun. Heat Mass Transf., 38(1), pp. 63–68. doi: 10.1016/j.icheatmasstransfer.2010.09.012

[12] Xie, G., Chen, Z., Sunden, B., Zhang, W., 2013. Comparative Study of the Flow and Thermal Performance of Liquid-Cooling Parallel-Flow and Counter-Flow Double-Layer Wavy Microchannel Heat Sinks. Numer. Heat Transf. Part A Appl., 64(1), pp. 30–55. doi: 10.1080/10407782.2013.773811.

[13] Sakanova, A., Zhao, J., Tseng, K. J., 2015. Investigation on the Influence of Nanofluids in Wavy Microchannel Heat Sink. IEEE Trans. Components, Packag. Manuf. Technol., 5(7), pp. 956–970. doi: 10.1109/tcpmt.2015.2441114.

[14] Saleem, S. and Heidarshenas, B., 2021. An investigation on exergy in a wavy wall microchannel heat sink by using various nanoparticles in fluid flow: two-phase numerical study. J. Therm. Anal. Calorim., 145(3), pp. 1599–1610. doi: 10.1007/s10973-021-10771-w.

[15] Ghorbani, N., Targhi, M. Z., Heyhat, M. M., Alihosseini, Y., 2022. Investigation of wavy microchannel ability on electronic devices cooling with the case study of choosing the most efficient microchannel pattern. Sci. Reports, 12, 5882. doi: 10.1038/s41598-022-09859-6.

[16] Devi, N. R., Moolya, S., Öztop, H. F., Abu-Hamdeh, N., Padmanathan, P., Satheesh, A., 2022. A review on ferrofluids with the effect of MHD and entropy generation due to convective heat transfer. Eur. Phys. J. Plus, 137(4), pp. 1–30. doi: 10.1140/epjp/s13360-022-02616-8.

[17] Zitouni, K., Aidaoui, L., Lasbet, Y., Tayebi, T., 2023. Entropy Generation-Based Analysis of Laminar Magneto-Convection in Different Cross-Section Channel Filled with Ferrofluid and Subjected to Partial and Full Magnetic Fields. J. Nanofluids, 12(5), pp. 1275–1297. doi: 10.1166/jon.2023.2013.

[18] Kumar, M. D., Jawad, M., Ramanuja, M., Ghodhbani, R., Yook, S. J., Abdallah, S. A. O., 2025. Forecasting heat and mass transfer enhancement in magnetized non-Newtonian nanofluids using Levenberg-Marquardt algorithm: influence of activation energy and bioconvection. Mech. Time-Dependent Mater., 29(1), pp. 1–24. doi: 10.1007/s11043-024-09739-8.

[19] Kumar, M. D., Gurram, D., Yook, S. J., Raju, C. S. K., Shah, N. A., 2025. Optimising thermal performance of water-based hybrid nanofluids with magnetic and radiative effects over a spinning disc. Chemom. Intell. Lab. Syst., 258, p. 105336. doi: 10.1016/j.chemolab.2025.105336.

[20] Kumar, M. D., Raju, C. S. K., Sajjan, K., Dharmaiah, G., Shah, N. A., Yook, S. J., 2025. Deep neural network-based prediction and computational fluid dynamics analysis of convective heat transfer in dusty fluid flow over heated surface. Phys. Fluids, 37(2). doi: 10.1063/5.0250396/3334189.

[21] Kumar, M. D., Raju, C. S. K., Shah, N. A., Yook, S. J., Gurram, D., 2025. Support vector machine learning classification of heat transfer rate in tri-hybrid nanofluid over a 3D stretching surface with suction effects for water at 10°C and 50°C. Alexandria Eng. J., 118, pp. 556–578. doi: 10.1016/j.aej.2025.01.061.

[22] Hamzah, H., Albojamal, A., Sahin, B., Vafai, K., 2021. Thermal management of transverse magnetic source effects on nanofluid natural convection in a wavy porous enclosure. J. Therm. Anal. Calorim., 143(3), pp. 2851–2865. doi: 10.1007/s10973-020-10246-4.

[23] Sohail, M., El-Zahar, E. R., Mousa, A. A., Nazir, U., Althobaiti, S., Althobaiti, A., Shah, N. A., Chung, J. D., 2022. Finite element analysis for ternary hybrid nanoparticles on thermal enhancement in pseudo-plastic liquid through porous stretching sheet. Sci. Reports, 12, 9219. doi: 10.1038/s41598-022-12857-3.

[24] Babu, M. J., Rao, Y. S., Kumar, A. S., Raju, C. S.K., Shehzad, S. A., Ambreen, T., Shah, N. A., 2022. Squeezed flow of polyethylene glycol and water based hybrid nanofluid over a magnetized sensor surface: A statistical approach. Int. Commun. Heat Mass Transf., 135, p. 106136. doi: 10.1016/j.icheatmasstransfer.2022.106136.

[25] Zhang, K., Shah, N. A., Alshehri, M., Alkarni, S., Wakif, A., Eldin, S. M., 2023. Water thermal enhancement in a porous medium via a suspension of hybrid nanoparticles: MHD mixed convective Falkner's-Skan flow case study. Case Stud. Therm. Eng., 47, p. 103062. doi: 10.1016/j.csite.2023.103062.

[26] Shah, N. A., 2025. Stagnation point on the micropolar bioconvection nanofluid flow over inclined Riga plate: Keller box analysis. Phys. Fluids, 37(1). doi: 10.1063/5.0250554/3329641.

[27] Cho, C. C., Chiu, C. H., Lai, C. Y., 2016. Natural convection and entropy generation of Al2O3–water nanofluid in an inclined wavy-wall cavity. Int. J. Heat Mass Transf., 97, pp. 511–520. doi: 10.1016/j.ijheatmasstransfer.2016.01.078.

[28] Mamourian, M., Milani Shirvan, K., Ellahi, R., Rahimi, A. B., 2016. Optimization of mixed convection heat transfer with entropy generation in a wavy surface square lid-driven cavity by means of Taguchi approach. Int. J. Heat Mass Transf., 102, pp. 544–554. doi: 10.1016/j.ijheatmasstransfer.2016.06.056.

[29] Asadi, A., Hossein Nezhad, A., Sarhaddi, F., Keykha, T., 2019. Laminar ferrofluid heat transfer in presence of non-uniform magnetic field in a channel with sinusoidal wall: A numerical study. J. Magn. Magn. Mater., 471, pp. 56–63. doi: 10.1016/j.jmmm.2018.09.045.

[30] Aidaoui, L., Lasbet, Y., Selimefendigil, F., 2020. Improvement of transfer phenomena rates in open chaotic flow of nanofluid under the effect of magnetic field: Application of a combined method. Int. J. Mech. Sci., 179, p. 105649. doi: 10.1016/j.ijmecsci.2020.105649.

[31] Aidaoui, L., Lasbet, Y., Selimefendigil, F., 2022. Effect of simultaneous application of chaotic laminar flow of nanofluid and non-uniform magnetic field on the entropy generation and energetic/exergetic efficiency. J. Therm. Anal. Calorim., 147(10), pp. 5865–5882. doi: 10.1007/s10973-021-10905-0.

[32] Kenniche, S., Aidaoui, L., Lasbet, Y., Boukhalkhal, A. L., Loubar, K., 2024. Simulation of enhancement techniques impact on fluid dynamics and thermal mixing of laminar forced convection flow. J. Therm. Anal. Calorim., 149(12), pp. 6265–6280. doi: 10.1007/s10973-024-13176-7.

[33] Tumse, S., Zontul, H., Hamzah, H., Sahin, B., 2023. Numerical Investigation of Magnetohydrodynamic Forced Convection and Entropy Production of Ferrofluid Around a Confined Cylinder Using Wire

Magnetic Sources. Arab. J. Sci. Eng., 48(9), pp. 11591–11620. doi: 10.1007/s13369-022-07470-5.

[34] Brinkman, H. C., 1952. The Viscosity of Concentrated Suspensions and Solutions. J. Chem. Phys., 20(4), p. 571. doi: 10.1063/1.1700493.

[35] Maxwell, J. C., 2010. A Treatise on Electricity and Magnetism. Cambridge University Press., doi: 10.1017/cbo9780511709340.

[36] Pirmohammadi, M., and Ghassemi, M., 2009. Effect of magnetic field on convection heat transfer inside a tilted square enclosure. Int. Commun. Heat Mass Transf., 36(7), pp. 776–780. doi: 10.1016/j.icheatmasstransfer.2009.03.023.

[37] Selimefendigil, F., and Öztop, H. F., 2014. Numerical study of MHD mixed convection in a nanofluid filled lid driven square enclosure with a rotating cylinder. Int. J. Heat Mass Transf., 78, pp. 741–754. doi: 10.1016/j.ijheatmasstransfer.2014.07.031.

[38] Moghadassi, A., Ghomi, E., Parvizian, F., 2015. A numerical study of water based Al2O3 and Al2O3–Cu hybrid nanofluid effect on forced convective heat transfer. Int. J. Thermal Sciences., 92, pp. 50–57. doi: 10.1016/j.ijthermalsci.2015.01.025.